Z. Phys. B – Condensed Matter 82, 211–216 (1991)

Condensed Matter
Zeitschrift für Physik B

Phase diagram of $LaTiO_x$: from 2D layered ferroelectric insulator to 3D weak ferromagnetic semiconductor

F. Lichtenberg[1], D. Widmer[1], J.G. Bednorz[1], T. Williams[2]*, and A. Reller[2]

[1] IBM Research Division, Zurich Research Laboratory, Säumerstrasse 4, CH-8803 Rüschlikon, Switzerland
[2] Institute for Inorganic Chemistry, University of Zurich, Winterthurerstrasse 190, CH-8057 Zürich, Switzerland

Received August 31, 1990

$LaTiO_x$ compounds are structurally related to perovskites and there are two known phases. The first, $x=3.50$, is a 2D layered-type ferroelectric. The second, $x=3.00$, is a weak ferromagnet with a 3D orthorhombic distorted perovskite structure. 20 samples with varying oxygen stoichiometry between these end members were prepared by floating zone melting, and then characterized by means of X-ray powder diffraction, electron microscopy, thermogravimetric analysis, resistivity and magnetic measurements. A phase diagram is established which displays the following physical and structural properties. A structural phase boundary at $x=3.20$ separates a new series of 2D layered structures from the 3D orthorhombic one. The former series represents the first conducting titanium oxides with a 2D layered structure to be reported. At $x=3.10$ a phase boundary exists between a metallic and a weak ferromagnetic state where the magnetic transition temperature T_c can be sensitively tuned by the oxygen stoichiometry x. Samples with T_c between 100 K and 130 K exhibit a metal-semiconductor transition whereas samples with higher T_c, up to 149 K, are semiconductors between room temperature and 4.2 K.

1. Introduction

Depending on the actual cation ratio, many phases with different structures exist in the La-Ti-O system. In most of them the titanium ion is four-valent, but interesting transport and magnetic properties are expected only for smaller valencies (non-empty 3d bands). This is known for many titanium compounds, e.g. $SrTiO_{3-y}$ which is an insulator for $y=0$ (valency $+4$) and is metallic and superconducting at very low temperatures for $y>0$ (valency smaller than $+4$). Only two examples with titanium valency smaller than $+4$ in the La-Ti-O system are known: $LaTiO_3$ – which will be discussed later – and $La_{2/3+y}TiO_3$ with $0 \leqq y \leqq 1/3$ [1]. In the La-Ti-O system with La/Ti = 1, two defined compounds, $LaTi^{+4}O_{3.5}$ and $LaTi^{+3}O_3$, with completely different physical and structural properties are known, and one can expect to control the titanium valency between $+4$ and $+3$ by changing only the oxygen stoichiometry. The first one, $La_2Ti_2O_7$ [2–4], is the ferroelectric with the highest known transition temperature of 1770 K [5]. Its 2D layered structure is monoclinic, based on parallel perovskite-type slabs of distorted TiO_6 octahedra connected by La and containing eight formula units of $LaTiO_{3.5}$ per unit cell [2]. The physical properties of the second one, $LaTiO_3$, however, depend on the oxygen stoichiometry and therefore on preparation conditions. Its structure had previously been determined to be a simple cubic perovskite but it is now established as a distorted orthorhombic perovskite ($GdFeO_3$ structure) containing four formula units per unit cell [6–8]. The physical properties of nominal $LaTiO_3$ have variously been determined to be a paramagnetic metal [9, 10] or a weak ferromagnet with $T_c=125$ K [6, 11] or 110 K [12] which displays a metal-semiconductor transition at 125 K [6]. Antiferromagnetic ordering of nominal $LaTiO_3$ was confirmed by neutron powder diffraction [11]. From the small effective moment found by magnetization measurements, it was concluded that the spins had to be canted to explain the weak ferromagnetism [11]. By changing the oxygen stoichiometry x in a systematic way, we can show that the different properties mentioned above are only part of a complex phase diagram.

2. Experimental

Starting materials were La_2O_3 (Th. Goldschmid AG or Molycorp, 99.99%), TiO_2 (JMC, Puratronic) and TiO (Alfa, optical grade, minimum purity 99%). Before using the La_2O_3, it was fired at 1100 °C in air and subsequently stored in dry atmosphere to prevent $La(OH)_3$ formation. In accordance with the formula

$$\tfrac{1}{2}\,La_2O_3 + (3.5-x)TiO + (x-2.5)TiO_2 \rightarrow LaTiO_x$$

* *Present address*: CSIRO Division of Materials Science and Technology, Locked Bag 33, Clayton, Victoria 3168, Australia

the starting materials were weighted with an accuracy of 1 mg to a total weight of about 8 g. After grinding, the powder was mixed with ethanol and pressed into two rods of 5 mm diameter and about 10 and 100 mm length, respectively. The rods were sintered on Al_2O_3 boats under flowing argon (purity 5.0) in a closed Al_2O_3 tube at 1400 °C whereby they usually became slightly oxidized ($\Delta x \simeq +0.04$). Afterwards the rods were melted under argon using the floating zone process in an elliptical mirror cavity with focussed infrared radiation. The rotation frequency of the seed part (small rod) and the zone speed were chosen to be 10 rpm and 15 mm/h, respectively.

The oxygen stoichiometry was determined by oxidizing the samples up to the stoichiometry of the end member $LaTiO_{3.5}$ and simultaneously measuring the increase in weight by means of a PERKIN-ELMER TAS-7 system thermomicrobalance. The uncertainty of the measurements was checked with a reference oxidation process and found to be $\leqq 1\%$.

In the range $3.20 < x < 3.40$ a second phase covers the melt-grown samples in the form of a thin surface layer. The volume fraction of this surface phase at $x \simeq 3.2$ is about 3% of the entire melt-grown sample, decreasing with increasing x and disappearing completely at $x = 3.40$. From thermogravimetric analysis we found that this second phase has a higher oxygen stoichiometry than the interior part of the sample. In the range $3.20 < x < 3.40$ structural and physical characterization was therefore performed only on the interior part of the melt-grown samples. For nominal oxygen stoichimetry between 3.20 and about 3.23 the samples lose oxygen during the preparation to give $x = 3.20$. Due to the usual slight oxidation which takes place for nominal x above 3.23, we have not yet been able to prepare samples with $x = 3.25$ and $x = 3.26$.

For the adjustment of the net oxygen stoichiometry between 3.50 and 3.00 the choice of appropriate ratios of TiO_2 and Ti metal as starting materials results in the same properties as using TiO and TiO_2. In contrast, a simple reduction process on the fully oxidized compound ($x = 3.50$) by zone melting under argon-hydrogen (ratio 96:4) atmosphere only leads to a lower limit of $x = 3.42$.

Resistivity measurements between room temperature and 4.2 K were made on rectangular bars cut from the melt-grown samples. The electrical contacts used in the four-wire method were made by silver paint and thin gold-beryllium or indium wires, and in selected cases were cross-checked with samples where the contact areas were sputtered with gold.

Magnetic measurements were taken on a SQUID susceptometer (S.H.E. model VTS 905) between room temperature and 2 K and in fields up to 5 Tesla. Small fields were determined each time by calibration with a standard lead sample. The raw materials La_2O_3, TiO_2 and TiO were checked separately and showed no indication of magnetic impurities.

Bulk structural analysis was performed by X-ray powder diffraction (SIEMENS Diffraktometer D 500) with CuKα radiation. High-resolution electron microscopy (HREM) and selected area electron diffraction (SAED) were used to investigate the microstructural and textural features using a PHILIPS CM 30 300 kV AEM as well as a JEOL 200 CX. For these investigations, fragments of crushed samples were deposited on copper grids coated with a holey-carbon film. Here we report first results concerning lattice parameters and symmetry; detailed structural work in progress will be published later.

3. Results and discussion

3.1. Structural investigations

X-ray powder diffraction and HREM at room temperature and thermogravimetric analysis reveal the existence of a series of distinct phases in the oxygen stoichiometry range $3.50 \geqq x \geqq 3.00$.

$LaTiO_{3.5}$ is monoclinic with lattice parameters $a = 7.80$ Å, $b = 5.55$ Å, $c = 13.0$ Å and $\beta = 98.6°$ which is in agreement with published results [2]. Upon lowering the oxygen stoichiometry a new series of monoclinic structures arises, including the possibility of varying the oxygen stoichiometry within the same structure. In the range $3.50 > x > 3.42$ it was revealed by HREM that intergrowth occurs between $LaTiO_{3.5}$ and a new phase with an ideal formula $LaTiO_{3.40}$. The latter exists in the range $3.42 \geqq x \geqq 3.40$, as shown by X-ray powder diffraction and HREM. A unit cell refinement of the powder data for $x = 3.40$ yields $a = 7.86$ Å, $b = 5.53$ Å, $c = 31.5$ Å and $\beta = 97.2°$ which is in agreement with values found by electron microscopy. HREM and SAED reveal that the monoclinic phases in the range $3.50 \geqq x \geqq 3.40$ are of 2D layered nature of which Fig. 1a shows a representative example. As found for $La_2Ti_2O_7$ and for the recently determined structure of the phase with an ideal formula $LaTiO_{3.40}$ [4], these 2D layered structures can be explained as being made up of perovskitic slabs connected by La cations. Thus the variable oxygen stoichiometries can be referred to the variation in the number of perovskitic TiO_6 octahedral layers constituting the slabs.

Samples with $x \leqq 3.20$ are orthorhombic. The distinction between a cubic and an orthohombic lattice could be made by electron diffraction. Although the diffraction patterns are well defined and reflect the orthorhombic symmetry, the HREM images reveal structural disorder on a microscopic level. This was observed in the entire orthorhombic range. A representative example, $x = 3.07$, is shown in Fig. 1b. Annealing of the sample with $x = 3.07$ for 12 h at 1400 °C in flowing argon showed that the HREM images remain unchanged. The lower the oxygen stoichimetry, the more difficult the separation of groups of X-ray diffraction peaks characteristic of the orthorhombic distortion. For $x \lesssim 3.15$ it was below the resolution of our diffraction system, but a least-squares refinement with a selected set of indexed lines leads to a convergent result. One finds that the unit cell volume increases with decreasing oxygen stoichiometry from $a = 5.56$ Å, $b = 5.55$ Å and $c = 7.87$ Å for $x = 3.20$ to $a = 5.62$ Å, $b = 5.61$ Å and $c = 7.92$ Å for $x = 3.00$. This is comparable to the results obtained from single crystals

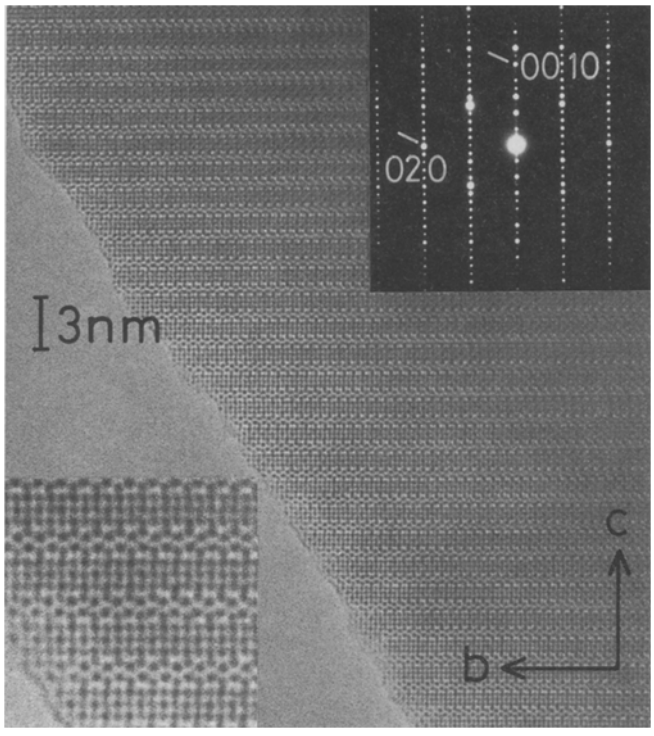

a

b

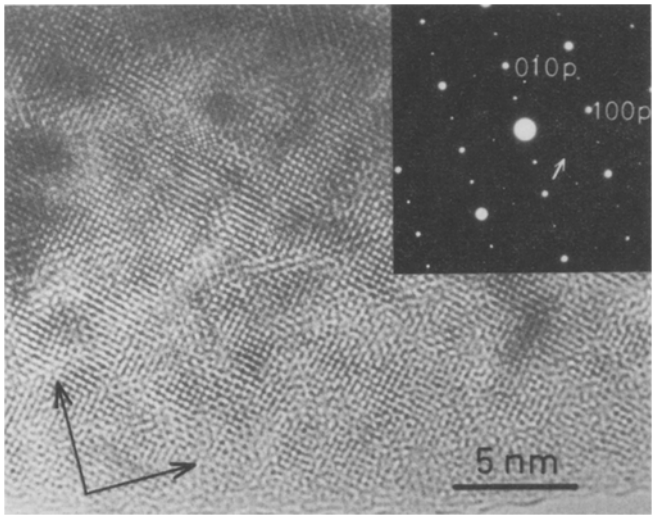

c

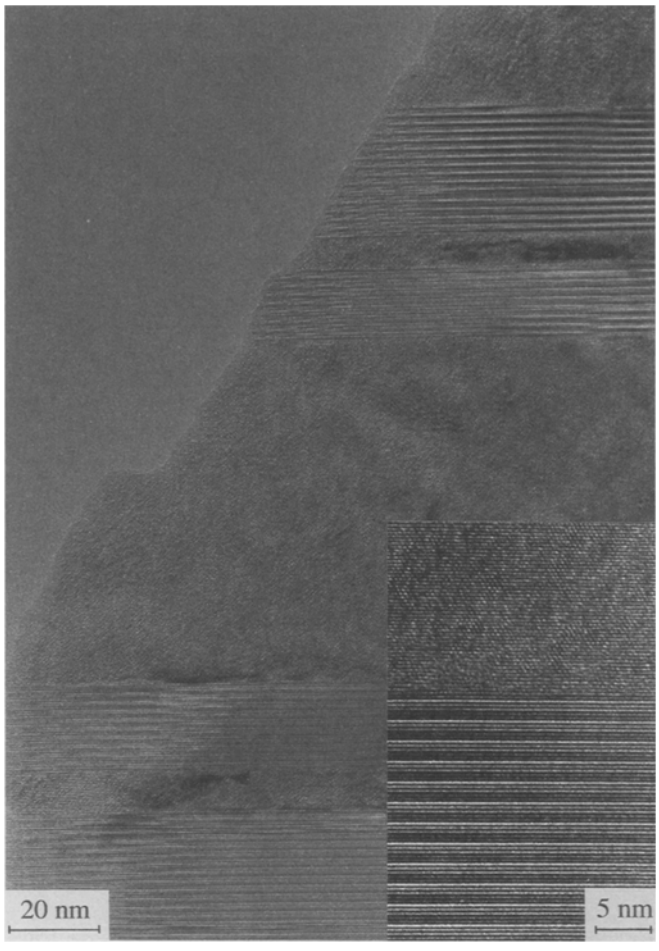

Fig. 1. **a** High-resolution lattice image from $LaTiO_{3.42}$ (a phase with ideal formula $LaTiO_{3.40}$ or $La_5Ti_5O_{17}$) taken with the incident 300 kV electron beam parallel with the [100] zone axis of the crystal. Inset at the top right ist the corresponding SAED pattern with the reflections 0, 2, 0 and 0, 0, 10 indicated. The five-metal-layers-thick perovskitic sheets run in parallel lines across the figure. The inset at bottom left shows the structure at higher magnification: the larger black spots correspond to columns of La atoms and the smaller spots to columns of Ti atoms (this is especially clear at the lower left of the inset, the thinnest region). Note the canting of metal atom rows in the adjacent layers. **b** HREM image and SAED pattern of 3D orthorhombic $LaTiO_{3.07}$ (projection along [001]). SAED reflections denoted $(100)_p$ as well as $(010)_p$ refer to the idealized cubic perovskite unit cell of $LaTiO_3$. The arrow indicates the position of the very weak reflection due to the orthorhombic symmetry. **c** HREM image displaying an intergrowth of the orthorhombic and monoclinic phases in a sample with the formal stoichiometry $LaTiO_{3.22}$. A highly magnified section of the intergrowth zone is shown as inset (bottom right)

of nominal $LaTiO_3$ with $a=5.60$ Å, $b=5.59$ Å and $c=7.91$ Å [7].

Intergrowth between the monoclinic layered and the orthorhombic structures was found by HREM in the range $3.20<x<3.29$ of which Fig. 1c shows a representative example. The crossover from $x=3.28$ to $x=3.29$ is accompanied by a large increase in the fraction of the monoclinic phase. This was found by X-ray powder diffraction and confirmed by HREM. For $3.29\leqq x<3.40$ a phase separation was revealed by HREM. In this range the 3D orthorhombic perovskite coexists with the 2D layered monoclinic structure of the type $LaTiO_{3.40}$. It was found by X-ray powder diffraction and confirmed by HREM that the monoclinic phase represents the majority and that the fraction of the orthorhombic phase diminishes with increasing x.

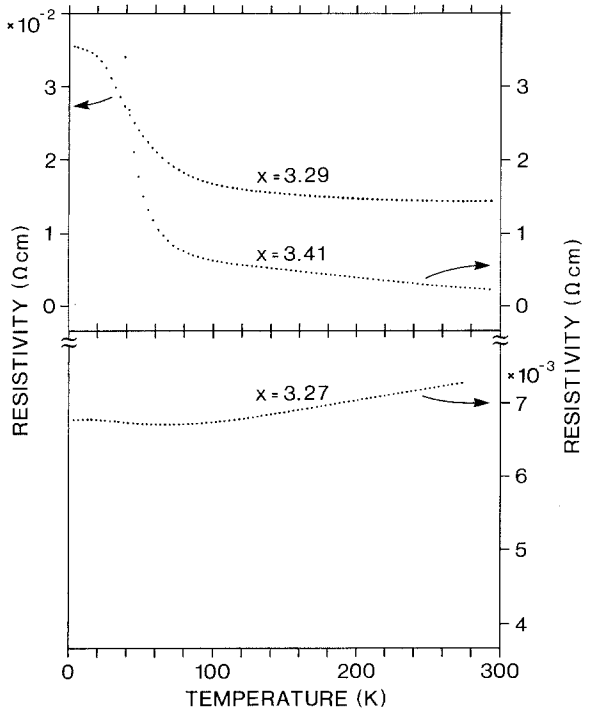

Fig. 2. Resistivity vs. temperature of selected samples of the range $3.50 > x > 3.20$

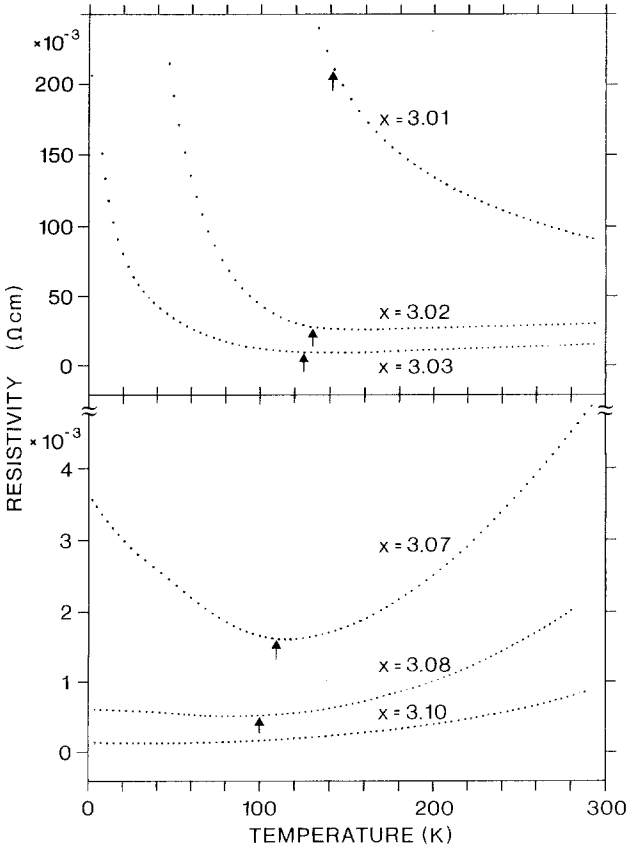

Fig. 3. Resistivity vs. temperature of selected orthorhombic samples. Arrows indicate the weak ferromagnetic transition temperature T_c as determined from susceptibility data (see text)

3.2. Physical properties

In the monoclinic region the resistivity decreases on lowering the oxygen stoichiometry x, at least within the same structure. Samples with $3.50 > x \geqq 3.40$ are semiconducting. Figure 2 shows the resistivity versus temperature of a sample with $x = 3.41$. To our knowledge these monoclinic phases represent the first conducting titanium oxides with a 2D layered structure to be reported. Semiconductivity was also found for $3.40 > x > 3.27$ of which Fig. 2 shows a representative example. The sample with $x = 3.27$, however, displays a weakly marked crossover from metallic to semiconducting behaviour at $T \simeq 70$ K (see Fig. 2). The sample with $x = 3.22$ is metallic down to 4.2 K. Although samples in the range $3.23 \leqq x \leqq 3.26$ have not yet been prepared, we expect that they are also metallic down to 4.2 K.

The orthorhombic samples are metallic in the range $3.10 \leqq x \leqq 3.20$ where at $x = 3.15$ the room temperature resistivity reaches 4×10^{-4} Ωcm, which is the smallest value in the system $LaTiO_x$. For $x \leqq 3.08$ the resistivity versus temperature displays a metal-semiconductor transition which disappears close to $x = 3.00$; samples with $x \leqq 3.01$ are semiconducting. A metal-semiconductor transition has already been observed at single crystals of nominal $LaTiO_3$ [6]. Figure 3 shows the temperature dependence of the resistivity of selected orthorhombic samples.

Low field susceptibility $\chi(T)$ was measured for samples with $x \leqq 3.42$ and with applied fields between 30 and 40 Gauss. For $x \geqq 3.10$, $\chi(T)$ displays a complex behavior which cannot be discussed within a simple physical picture. The most remarkable property is the appearance of a minimum in the temperature dependence of χ in the range $3.10 \leqq x \leqq 3.42$. The order of magnitude of $\chi(T)$ increases from 10^{-7} emu/gram × gauss for $x \simeq 3.42$ to 10^{-6} emu/gram × gauss for $x \simeq 3.10$.

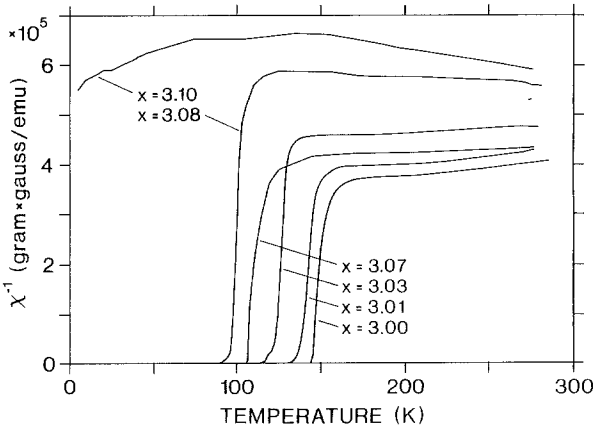

Fig. 4. Inverse low-field susceptibility vs. temperature of selected orthorhombic samples with $x \leqq 3.10$

$\chi^{-1}(T)$ and $\chi(T)$ of selected orthorhombic samples with $x \leqq 3.10$ are shown in Figs. 4 and 5, respectively.

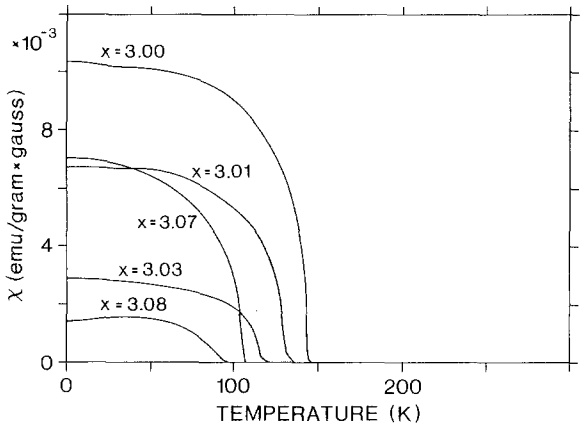

Fig. 5. Low-field susceptibility vs. temperature of selected orthorhombic samples with $x<3.10$

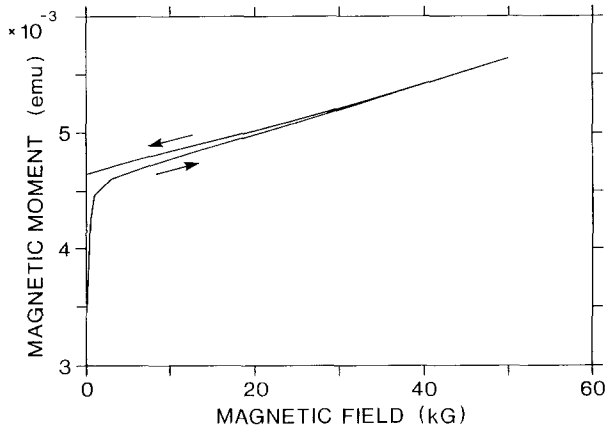

Fig. 6. Magnetization curve at $T=5$ K up to 50 kGauss for $x=3.00$ with start field of +5 Gauss and end field of −5 Gauss

The sample with $x=3.10$ is still metallic (see Fig. 3) and $\chi^{-1}(T)$ shows a maximum (see Fig. 4), but samples with $x\leqq 3.08$ display magnetic ordering (see Figs. 4 and 5) together with the already mentioned metal-semiconductor transition which disappears again for $x\leqq 3.01$ (see Fig. 3). The absolute value of χ depends on the perfection of the zone melting-grown samples, e.g. $x=3.07$ does not fit into the sequence (see Figs. 4 and 5). Defining the magnetic transition temperature T_c by the midpoint of the transition in Fig. 4, one finds that T_c increases from 100 K to 149 K by lowering the oxygen stoichiometry from $x=3.08$ to $x=3.00$. This is in accordance with the expectation that in the case of titanium the value of T_c should increase by lowering the valency and therefore by increasing the average number of $3d$ electrons. The temperature where the metal-semiconductor transition occurs (resistivity minimum) increases with increasing T_c from ~ 100 K ($x=3.08$, $T_c=100$ K) to ~ 165 K ($x=3.02$, $T_c=130$ K). When comparing only the T_c values, our samples with $x=3.07$ ($T_c=110$ K) and $x=3.03$ ($T_c=125$ K) correspond to nominal $LaTiO_3$ of [12] and [6], respectively. The behavior of $\chi^{-1}(T)$ for $T>T_c$ (see Fig. 4) and its extrapolation down to zero suggests that the nature of the magnetic ordering is related to antiferromagnetism, in accordance with the neutron powder diffraction result of nominal $LaTiO_3$ [11].

Weak ferromagnetism for all samples with $x\leqq 3.08$ was confirmed by measuring a half hysteresis loop at $T=5$ K. A representative example, $x=3.00$, is shown in Fig. 6. All samples have the following in common: remanence, linear behavior at high fields and no saturation up to 50 kGauss. The two latter properties are not in accordance with single crystal data of nominal $LaTiO_3$ [6]. To obtain a lower limit for the number of Bohr magnetons per formula unit, n_B, one can use the magnetic moment at 50 kGauss. This yields $n_B=0.01$ for $x=3.08$ ($T_c=100$ K) and $n_B=0.02$ for $x=3.00$ ($T_c=149$ K), which is of the same order of magnitude as found for single crystals of nominal $LaTiO_3$ [6]. The existence of the high field susceptibility (linear behavior for high fields, see Fig. 6) might indicate spin canting which leads to weak ferromagnetism [13].

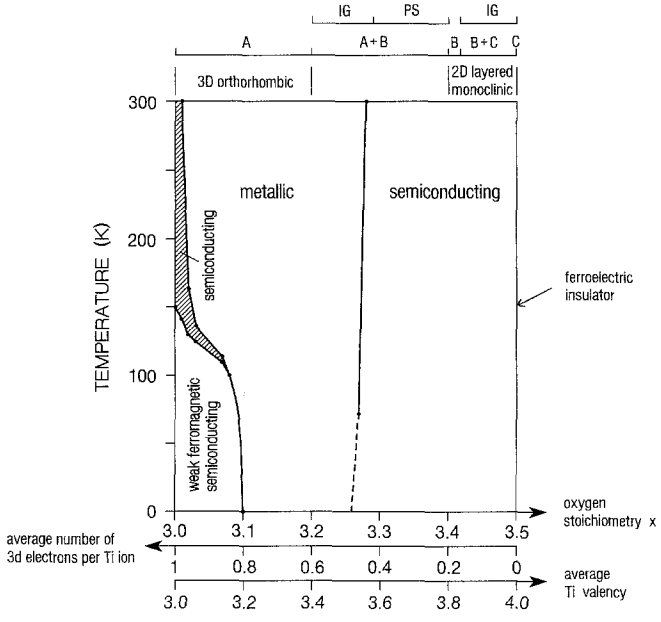

Fig. 7. Phase diagram of $LaTiO_x$ according to our present data. Structural statements refer to room temperature: A indicates the distorted perovskite, B the structure of $LaTiO_{3.40}$ and C the structure of $LaTiO_{3.50}$. IG indicates intergrowth and PS means phase separation between A and B, where B is the majority phase. Metallic and semiconducting refer to $d\rho/dT>0$ and $d\rho/dT<0$, respectively, where ρ is the resistivity. The average number of 3d electrons per Ti ion and the average Ti valency represent a linear interpolation based on a simple charge neutrality calculation

Many orthorhombically distorted perovskites display magnetic ordering like antiferromagnetism, weak ferromagnetism and ferromagnetism [14]. Ferromagnetic $SrRuO_3$, for example, is isomorphous with $LaTiO_3$; they have approximately the same T_c (160 K and 149 K, respectively) and no saturation of their magnetization at high fields [15, 16]. But in contrast to $LaTiO_3$, $SrRuO_3$ is metallic between 300 K and 4.2 K, its magnetization at high fields is nonlinear and its ferromagnetic ordering is due to itinerant electrons with $n_B=1.4$ [15, 16].

The above-mentioned structural disorder in the orthorhombic range therefore also concerns the weak ferromagnets. This raises again the question whether weak ferromagnetism in antiferromagnetic compounds is an intrinsic property or due to some structural irregularities, see e.g. [17] and references therein.

In Fig. 7 we present all our current results of $LaTiO_x$ in the form of a phase diagram displaying the surprising complexity arising by merely changing the oxygen stoichiometry. In the range $3.10 \geqq x \geqq 3.00$ the data points of the lower curve (magnetic transition temperature T_c) are obtained from magnetic measurements and those of the upper curve (metal-semiconductor transition) from resistivity measurements.

4. Conclusion

We have shown that a series of distinct phases with variable oxygen stoichiometry exist in the $LaTiO_x$ system in the range $3.50 \geqq x \geqq 3.00$. The phase diagram established shows that the structural and physical properties vary drastically with oxygen stoichiometry. Starting from the fully oxidized compound and then lowering the oxygen stoichiometry, the perovskite-related structure changes from a new series of 2D layered type – the first conducting titanium oxides with 2D layered structure to be reported – to a known 3D type. The corresponding physical properties vary from ferroelectric insulating to semiconducting, metallic and finally to a weak ferromagnetic state. The variation of properties in the latter, close to the composition of $LaTiO_3$, displays the highest sensitivity to x in the whole system, thus explaining the nonconverging results obtained in earlier work. By systematically varying x down to the limit at $x = 3.00$, the temperature driven metal-semiconductor transition disappears and the T_c of the weak ferromagnetism reaches its maximum of 149 K.

TBW sincerely thanks Professor H.R. Oswald, University of Zurich, and Professor G. Kostorz, ETH Zurich, for their hospitality and kind provision of electron microscope time and is grateful to the Swiss National Science Foundation (No. 2.838-085) for financial support. We wish to thank B. Spring for performing the thermogravimetric analysis and S. Alvarado and R. Allenspach for pertinent discussions and for critically reading the manuscript. Furthermore we wish to thank C. Rossel and J.D. Mannhart for critically reading the manuscript.

References

1. Moeller, C.W.: J. Chem. Phys. **27**, 983 (1957)
2. Gasperin, P.M.: Acta Crystallogr B**31**, 2129 (1975)
3. Schmalle, H., Williams, T., Reller, A., Bednorz, J.G.: Acta Crystallogr. (submitted for publication)
4. Williams, T., Schmalle, H., Reller, A., Lichtenberg, F., Widmer, D., Bednorz, J.G.: J. Solid State Chem. (submitted for publication)
5. Nanamatsu, S., Kimura, M., Doi, K., Matsushita, S., Yamada, N.: Ferroel. **8**, 511 (1974)
6. MacLean, D.A., Greedan, J.E.: Inorg. Chem. **20**, 1025 (1981)
7. MacLean, D.A., Hok-Nam Ng, Greedan, J.E.: J. Solid State Chem. **30**, 35 (1979)
8. Johnston, W.D., Sestrich, D.: J. Inorg. Nucl. Chem. **20**, 32 (1961)
9. Rogers, D.B., Ferretti, A., Ridgley, D.H., Arnott, R.J., Goodenough, J.B.: J. Appl. Phys. **37**, 1431 (1966)
10. Greedan, J.E., MacLean, D.A.: Inst. Phys. Conf. Ser. No. 37, 249 (1978)
11. Goral, J.P., Greedan, J.E.: J. Magn. Magn. Mater. **37**, 315 (1983)
12. Maeno, Y., Awaji, S., Matsumoto, H., Fujita, T.: Proceedings of the 19th International Conference on Low Temperature Physics, Sussex 1990
13. Goodenough, J.B.: Prog. Solid State Chem. **5**, 185 (1971)
14. Goodenough, J.B., Longo, J.M: In: Landolt-Boernstein New Series (Group III) 4, 126 (1970)
15. Bouchard, R.J., Gillson, J.L.: Mater. Res. Bull. **7**, 873 (1972)
16. Longo, J.M., Raccah, P.M., Goodenough, J.B.: J. Appl. Phys. **39**, 1327 (1968)
17. Watanabe, H.: J. Phys. Soc. Jpn. **14**, 511 (1959)